Effect of Magnetic Boundary Conditions on Superfluid ^{3}He in Nematic Aerogel

V. V. Dmitriev,[1,*] A. A. Soldatov,[1,2] and A. N. Yudin[1]
[1]P.L. Kapitza Institute for Physical Problems of RAS, 119334 Moscow, Russia
[2]Moscow Institute of Physics and Technology, 141700 Dolgoprudny, Russia

(Received 27 September 2017; revised manuscript received 19 December 2017; published 13 February 2018)

We report results of experiments with superfluid ^{3}He confined in aerogels with parallel strands which lead to anisotropic scattering of ^{3}He quasiparticles. We vary boundary conditions for the scattering by covering the strands with different numbers of atomic ^{4}He layers and observe that the superfluid phase diagram and the nature of superfluid phases strongly depend on the coverage. We assume the main reason for these phenomena is a magnetic channel of the scattering which becomes important at low coverages and can be essential in other Fermi systems with triplet pairing.

DOI: 10.1103/PhysRevLett.120.075301

Introduction.—In many Fermi systems, e.g., in liquid ^{3}He, in some cold atomic gases, and unconventional superconductors, a triplet Cooper pairing occurs resulting in superfluid (superconducting) states. An ideal object to study the effect of impurities on such states is ^{3}He: it has a spherical Fermi surface, its superfluid phases (A, B, A_1) in the bulk are well understood, and its superfluid coherence length can be varied by pressure in the range of 20–80 nm [1]. Although superfluid ^{3}He is originally pure, a well-defined system with impurity scattering can be obtained by immersing a high porosity aerogel in the fluid. In such experiments silica aerogels are typically used. At temperatures $T \sim 1$ mK, where ^{3}He is superfluid, the scattering of ^{3}He quasiparticles occurs only on aerogel strands. In pure ^{3}He, the strands are covered with ~2 atomic layers of paramagnetic solid ^{3}He [2–4] and the scattering is diffusive. Boundary conditions for the scattering may be varied by a small amount of ^{4}He which covers the strands with a few atomic layers and replaces solid ^{3}He. In this case the scattering is diffusive only if $P \geq 25$ bar while at low pressures it is specular or partly specular [5–9]. If the ^{4}He amount is enough to completely remove the solid ^{3}He, the spin is conserved during the scattering. In contrast, in pure ^{3}He the spin is not conserved due to a fast exchange between atoms of liquid and solid ^{3}He resulting in a spin-exchange (magnetic) scattering channel. However, experiments with silica aerogels show no clear evidence of the magnetic channel. In particular, the observed A-like and B-like phases correspond to A and B phases of bulk ^{3}He, regardless of the presence or absence of ^{4}He [10–16]. Moreover, the superfluid transition temperature of ^{3}He in aerogel (T_{ca}) is independent of the coverage at high pressures [10,14] while a small increase of T_{ca} in the presence of ^{4}He at lower pressures [17,18] is probably due to the change in specularity. In most theoretical models of ^{3}He in aerogel the magnetic channel is neglected (e.g., Refs. [19–23]), except in a few papers where its influence on the A phase [24], on the $A - A_1$ transition [25–27], and on the heat transport in the normal phase [28] is considered.

Presumably, the magnetic scattering in ^{3}He in silica aerogels is masked due to their small global anisotropy. In this case the scattering is nearly isotropic, regardless whether it is diffusive or specular, and an additional "randomization" due to the magnetic channel does not change the picture. The situation might be different for anisotropic scattering [23] but this has not been investigated. To obtain anisotropic scattering, a "nematic" aerogel (N-aerogel) [29] can be used. Its strands are nearly parallel, and at ultralow temperatures the effective mean free path of ^{3}He quasiparticles along the strands ($l_\parallel$) is longer than in the transverse direction ($l_\perp$) [30,31]. Theoretically, this enhances the appearance of new phases not existing in bulk ^{3}He, i.e., the polar, polar distorted A (denoted as DA), and polar distorted B (DB) phases [22,23,32,33]. These phases were recently observed in experiments with ^{3}He in N-aerogels [34–37]. We note that the aerogel strands in Refs. [34–36] were covered by ^{4}He to remove the paramagnetic ^{3}He.

In this work we describe experiments on ^{3}He in N-aerogels with pure ^{3}He and with the strands covered by different numbers of atomic ^{4}He layers. We show that even a small amount of paramagnetic ^{3}He on the strands drastically changes the superfluid phase diagram.

Samples and methods.—We used four samples of N-aerogel with different porosities (see Table I). They have a cuboid shape with sizes of ≈4 mm and were prepared from a new material "nafen" (produced by ANF Technology) which consists of Al_2O_3 strands with diameters ≈9 nm.

The necessary low temperatures were obtained with a nuclear demagnetization cryostat and were determined using a quartz tuning fork. Measurements were performed using continuous wave (cw) NMR in magnetic fields

TABLE I. Characteristics of the samples: ρ is the overall density, d is the mean distance between axes of adjacent strands.

Sample	ρ (mg/cm^3)	Porosity (%)	d (nm)	$l_\parallel$ (nm)	$l_\perp$ (nm)
nafen-72	72	98.2	64	⋯	⋯
nafen-90	90	97.8	58	960	290
nafen-243	243	93.9	35	570	70
nafen-910[a]	910	78	18	⋯	⋯

[a]Prepared from nafen with density 72 mg/cm^3 (see Ref. [38]).

2.4–27.8 mT (the corresponding NMR frequencies are 78–902 kHz) and at pressures 0.2–29.3 bar. An external magnetic field $\mathbf{H}$ could be oriented at any angle μ with respect to the direction of the nafen strands ($\hat{\zeta}$).

To obtain the ^{4}He coverage we added ^{4}He (1.35 or 1.55 mmole) into the empty experimental cell at $T \leq 100$ mK and then filled the cell with ^{3}He. The area of the experimental region is dominated by a sintered silver powder heat exchanger to cool the ^{3}He. The exchanger area estimated from the powder grain size is ~40 m^2 [39] (the area of the samples in the cell is ~1 m^2 [29]), and the used ^{4}He amounts should correspond to 2.2 and 2.5 atomic ^{4}He layers (called below 2.2 coverage and 2.5 coverage). These numbers are approximate because the area may be smaller by 10%–30% due to sintering [40]. For the purpose of this Letter it is more important that the 2.5 coverage corresponds to the minimal ^{4}He amount which results in the absence of the paramagnetic NMR signal from ^{3}He up to $P = 29.3$ bar. We note that the samples were not damaged during the filling of the cell and had surfaces with equal ^{4}He coverage (see the Supplemental Material [41]).

Identification of superfluid phases.—Depending on conditions we observed the polar, *DA*, *A*, *DB*, or *B* phase. The polar, *DA*, and *A* phases are equal spin pairing (ESP) phases whose spin susceptibilities equal the normal phase value. In the *DB* and *B* phases the susceptibility is smaller. This makes it easy to distinguish between these two groups of phases. On cooling from the normal phase, the transition occurred into the ESP phases and then (if it took place)—into the *DB* or *B* phases [low temperature (LT) phases]. The superfluid phases were identified from their NMR properties which depend on the order parameter, its spatial distribution, and μ. In particular, we measured the dependencies of a cw NMR frequency shift ($\Delta\omega$) from the Larmor frequency ($\omega_L = \gamma H$) on T and μ. The LT phases were identified by comparing $\Delta\omega$ at $\mu = 0$ (where $\Delta\omega$ is maximal) with the maximal shift in bulk ^{3}He-*B* and also by measurements at $\mu = 90°$ (see Ref. [35] for NMR properties of the *DB* phase). In this Letter we focused on measurements in the ESP phases. Below we consider their properties in more detail.

The general form of the order parameter of these phases is

$$A_{\nu k} = \Delta_0 e^{i\varphi} d_\nu (a m_k + i b n_k), \tag{1}$$

where Δ_0 is the gap parameter, φ is the phase, $a^2 + b^2 = 1$, $\mathbf{d}$ is the unit spin vector oriented normal to the magnetization, $\mathbf{m}$ and $\mathbf{n}$ are mutually orthogonal unit orbital vectors. The *DA* phase ($a^2 > b^2 > 0$) is an intermediate state between the polar ($a = 1$, $b = 0$) and *A* phases ($a = b$). *N*-aerogel strands fix $\mathbf{m} \| \hat{\zeta}$ [22] and destroy long-range order in the *DA* and *A* phases, where $\mathbf{n}$ is random at distances larger than ~1 μm forming a static 2D Larkin-Imry-Ma state [34,45,46]. The order parameter of the polar phase does not contain $\mathbf{n}$. It makes this phase topologically different from the *DA* and *A* phases: it is not chiral, and its gap is zero in the plane normal to $\mathbf{m}$.

In the ESP phases a uniform spatial distribution of $\mathbf{d}$ is favored (spin nematic, SN, state) and the dipole energy $U_D \propto [a^2(\mathbf{dm})^2 + b^2(\mathbf{dn})^2]$ results in the following cw NMR shift:

$$2\omega_L \Delta\omega = \Omega_\parallel^2 \cos^2 \mu, \tag{2}$$

where $\Omega_\parallel = \Omega_\parallel(P, T)$ is the longitudinal resonance frequency (which is ~100 kHz at $T = 0$ and 0 at $T = T_{ca}$) and can be expressed in terms of the Leggett frequency of the *A* phase: $\Omega_\parallel^2 = K\Omega_A^2$, where in the *A* phase $K = 1/2$ while in the polar and *DA* phases in the weak-coupling limit K should equal 4/3 and $(4–6b^2)/(3–4a^2b^2)$ correspondingly. However, this limit is a good approximation only at low pressures [1]. Experimentally it was found that in the polar phase $K = K_p(P)$ decreases from 4/3 to ≈1.15 while increasing pressure from 2.9 to 29.3 bar, independently of the nafen porosity [36]. Consequently, if Ω_A is known, measurements of $\Delta\omega$ allow us to determine K and identify the ESP phase. Fortunately, in most of our experiments $\Delta T_{ca} = T_c - T_{ca} \ll T_c$, where T_c is the transition temperature in bulk ^{3}He. In this case Ω_A can be found by rescaling the Leggett frequency (Ω_{A0}) of bulk ^{3}He-*A*: $\Omega_A(T/T_{ca})/\Omega_{A0}(T/T_c) = T_{ca}/T_c$.

An additional property used for the identification is that in the *DA* and *A* phases (but not in the polar phase), a metastable spin glass (SG) state with random $\mathbf{d}$ may exist. This state corresponds to a local energy minimum and is stabilized by the random $\mathbf{n}$ field due to the dipole interaction. It can be created by cooling through T_{ca} in the presence of high NMR excitation generating a random $\mathbf{d}$ distribution [15]. A distinctive feature of the SG state is that at $\mu = 90°$ the NMR shift is negative while in the SN state it equals 0 [36].

It follows from Eq. (2) that $\Delta\omega$ is maximal at $\mu = 0$. Therefore, we usually detected T_{ca} at $\mu = 0$ from the appearance of a nonzero NMR shift ($\Delta\omega_0$). From measurements of $\Delta\omega_0 = \Delta\omega_0(T)$ we then determined K and identified the phases assuming that in the polar phase $K = K_p$, in the DA phase $1/2 < K < K_p$, and in the *A*

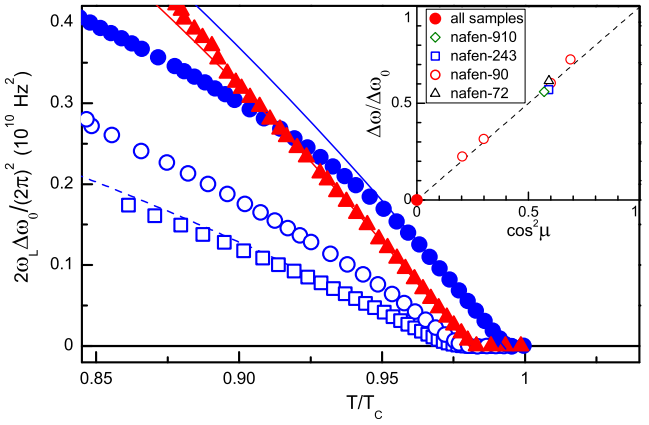

FIG. 1. cw NMR frequency shifts versus temperature at $P = 29.3$ bar in SN states for $\mu = 0$. Filled circles: nafen-72 (2.5 coverage, $T_{ca} = 0.993T_c$). Triangles: nafen-243 (2.5 coverage, $T_{ca} = 0.981T_c$). Open circles: nafen-72 (2.2 coverage, $T_{ca} = 0.977T_c$). Squares: nafen-72 (pure ^{3}He, $T_{ca} = 0.974T_c$). Solid lines: theory for the polar phase ($K = 1.15$). Dashed line: theory for the A phase. (Insert) $\Delta\omega/\Delta\omega_0$ versus μ in the SN state measured at different temperatures and pressures. Dashed line is Eq. (2).

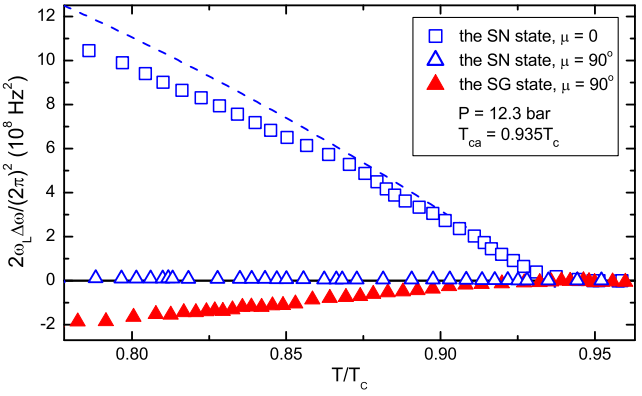

FIG. 2. cw NMR frequency shifts versus temperature with pure ^{3}He in nafen-90. Dashed line: theory for the A phase for $\mu = 0$.

phase $K = 1/2$. Measurements of $\Delta\omega$ at arbitrary μ were also performed and agreed well with Eq. (2) (see insert in Fig. 1).

We note that when solid ^{3}He covers the aerogel strands the NMR frequency is a weighted average of NMR frequencies of liquid and solid ^{3}He due to the fast exchange mechanism [4,47]. The magnetization of paramagnetic ^{3}He follows the Curie-Weiss law, and at $T \sim T_c$ its total magnetic moment (M_s) may exceed that of liquid ^{3}He (M_l). For example, for pure ^{3}He in nafen-243 at 7.1 bar $M_s/M_l \approx 2.7$ at $T = T_c$. Therefore, to compare the experimental data with Eq. (2) the observed shift was corrected using the measured temperature dependence of M_s/M_l.

Results with pure ^{3}He *and for 2.5 coverage.*—In Fig. 1 we show the temperature dependencies of $\Delta\omega_0$ for ^{3}He in nafen-72 (filled circles) and nafen-243 (triangles) for the 2.5 coverage. At $0.96T_c < T < T_{ca}$ the shift for nafen-72 follows the curve with the same slope as for nafen-243 ($K = K_p = 1.15$) that corresponds to the polar phase. Below $0.96T_c$ the data deviate from the curve due to the second order transition into the DA phase, similar to that observed earlier with nafen-90 [36]. In the same figure the data for pure ^{3}He in nafen-72 are plotted with squares. They nearly follow the curve expected for the A phase (the discrepancy is probably due to systematic errors in measurements of M_s/M_l).

In nafen-90 and nafen-243 we observed similar differences between the 2.5 coverage and pure ^{3}He: for the 2.5 coverage the superfluid transition occurred into the polar phase while in pure ^{3}He this phase was no longer observed. In Fig. 2 we show the data for $\Delta\omega_0$ in nafen-90 (squares) which are close to the curve for the A phase. Additionally, with pure ^{3}He in this sample (as well as in nafen-72 and nafen-243) the SG state was easily created (filled triangles in Fig. 2) confirming the absence of the polar phase. In contrast, at 2.5 coverage all attempts to create the SG state in these samples failed.

Based on the present measurements, the superfluid phase diagrams of ^{3}He in nafen-72 for 2.5 coverage and with pure ^{3}He are shown in Fig. 3 (see the Supplemental Material [41] for the diagrams in nafen-90 and nafen-243). With pure ^{3}He in all samples the polar phase no longer exists and ΔT_{ca} is essentially greater than for the 2.5 coverage. This additional suppression of T_{ca} increases with decreasing nafen porosity. It is especially clear in nafen-910: with pure ^{3}He the superfluid transition was not detected down to the lowest attained temperatures ($\approx 0.25T_c$ at 29.3 bar) but at the 2.5 coverage the transition was observed (Fig. 4). In this case ΔT_{ca} is too large and Ω_A cannot be determined by rescaling Ω_{A0}. However, we believe that the transition occurs into the polar phase. First, our attempts to create the SG state failed. Second, we were able to create half-quantum vortices in this phase. As shown in previous experiments [48], such vortices can be created in the polar phase by a fast cooling through T_{ca} owing to the Kibble-Zurek mechanism. They survive in nafen due to pinning and result in a satellite NMR peak with a frequency shift $\Delta\omega_{\rm sat} = \Delta\omega_0(\cos^2\mu - \lambda\sin^2\mu)$, where $\lambda \leq 1$. The insert in Fig. 4 shows the NMR spectrum with nafen-910 after a rapid cool down. The satellite peak position corresponds to $\lambda = 0.93$ in agreement with Ref. [48].

These observations allow us to affirm that with pure ^{3}He the superfluid transition occurs into the A phase (or, probably, into the DA phase in nafen-243) while at 2.5 coverage—into the polar phase. In nafen-72 and nafen-90 at low enough temperatures we observed a first order transition into the LT phase whose properties at 2.5 coverage correspond to the DB phase. With pure ^{3}He the LT phase is close to the B phase but due to a very wide

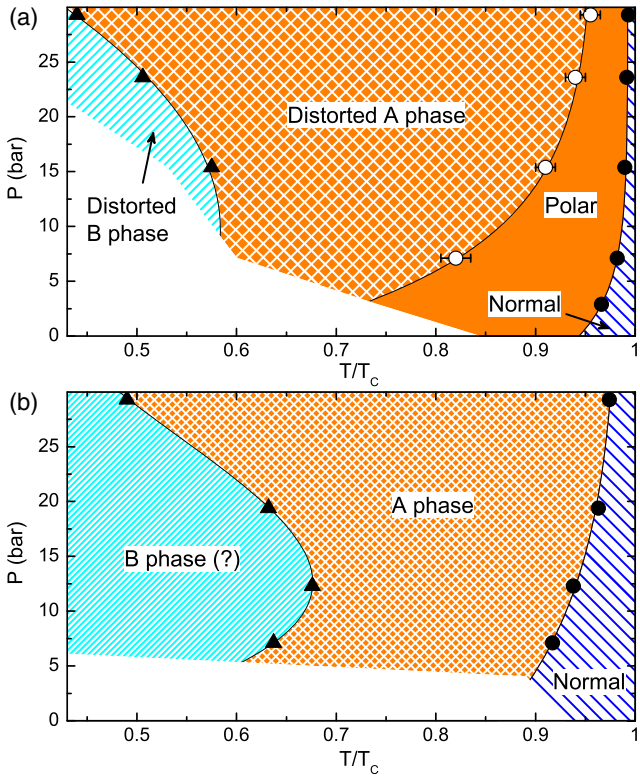

FIG. 3. Phase diagrams of ^{3}He in nafen-72 for 2.5 coverage (a) and for pure ^{3}He (b) obtained on cooling from the normal phase. Filled circles mark T_{ca}. Open circles mark the transition between the polar and *DA* phases. Triangles mark the beginning of the transition into the *DB* (or *B*) phase. The white area shows regions with no experimental data. The *x* axis represents the temperature normalized to the superfluid transition temperature of bulk ^{3}He.

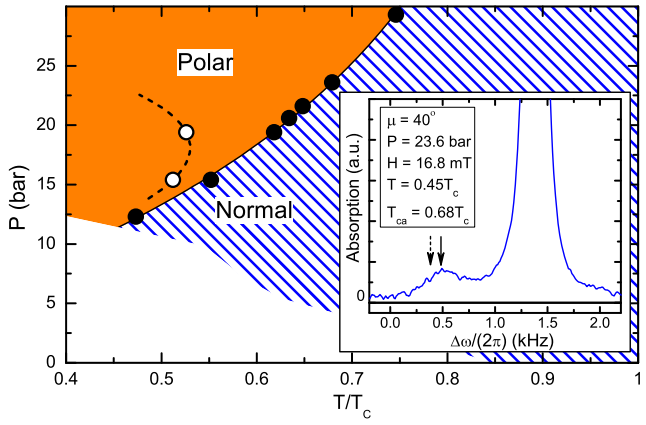

FIG. 4. Phase diagram of ^{3}He in nafen-910. Filled circles mark the superfluid transition of ^{3}He for 2.5 coverage. Open circles mark the transition for 2.2 coverage. Dashed line is a guide to the eye, but it takes into account that at $P = 29.3$ bar no transition was observed for 2.2 coverage down to $\approx 0.3T_c$. (Insert) cw NMR absorption with the satellite peak from half-quantum vortices in ^{3}He in nafen-910 for 2.5 coverage. Arrows mark the expected position of the satellite peak for $\lambda = 0.93$ (solid arrow) and $\lambda = 1$ (dashed arrow).

NMR line in this state its properties were not measured with sufficient accuracy.

Results for 2.2 coverage.—With ^{3}He in nafen-910 for the 2.2 coverage we detect no signal from the paramagnetic ^{3}He at any pressure except 29.3 bar, where it was small and corresponded to ~0.1 atomic layers of solid ^{3}He. However, the superfluid transition was not found down to the lowest attained temperature ($\approx 0.3T_c$). At lower pressures the transition was observed (open circles in Fig. 4) but T_{ca} was more suppressed than at the 2.5 coverage. We explain such unusual pressure dependence of T_{ca} by the following. It is known that the ^{4}He amount which is enough to remove solid ^{3}He from the surface decreases with decreasing pressure [7]. Therefore, at low pressures the 2.2 coverage is enough to completely remove the paramagnetic ^{3}He. Above ≈15 bar a small amount of solid ^{3}He appears and ΔT_{ca} increases. This amount grows with increasing pressure [2–4], and at 29.3 bar, where the paramagnetic signal is already detectable, ΔT_{ca} becomes so large that we cannot even reach T_{ca}.

With nafen-72, placed in the same chamber, the paramagnetic signal was not detected even at 29.3 bar due to a smaller surface area of the sample. However, the effect of solid ^{3}He was also clear: the temperature dependence of $\Delta\omega_0$ (open circles in Fig. 1) corresponds to the *DA* phase even near T_{ca}, where $K \approx 0.75$. The influence of solid ^{3}He in nafen-72 is seen down to ≈15 bar but at lower pressures no differences between 2.2 and 2.5 coverages were found. It is worth mentioning that together with these experiments we also investigated the behavior of the quartz tuning fork. It was found that the resonance properties of the fork are also sensitive to the presence of solid ^{3}He [49].

Conclusions.—We observe that even a very small amount of paramagnetic ^{3}He on nafen strands drastically changes the superfluid phase diagram of ^{3}He in nafen: on cooling from the normal phase the superfluid transition occurs into the *DA* or *A* phases while in absence of paramagnetic ^{3}He the transition occurs into the polar phase. Solid ^{3}He on the strands also essentially reduces T_{ca}, especially in low porosity nafen, where the scattering anisotropy is greater. The observed phenomena cannot be explained by a change of the scattering specularity because they are observed also at high pressures where the scattering should be diffusive regardless of the presence or absence of solid ^{3}He. The only explanation we can suggest is the importance of a magnetic channel in the presence of strong anisotropy in the ^{3}He quasiparticle scattering. We hope that our results will stimulate further theoretical studies of this phenomenon on triplet superfluidity.

We are grateful to I. M. Grodnensky for providing nafen samples, V. P. Mineev, M. Krusius, J. A. Sauls, and G. E.

Volovik for useful discussions and comments. This work was supported in part by RFBR (Grant No. 16-02-00349) and by Basic Research Program of the Presidium of Russian Academy of Sciences.

*dmitriev@kapitza.ras.ru

[1] D. Vollhardt and P. Wölfle, *The Superfluid Phases of Helium 3* (Taylor & Francis, London, 1990).
[2] A. Schuhl, S. Maegawa, M. W. Meisel, and M. Chapellier, Phys. Rev. B **36**, 6811 (1987).
[3] J. A. Sauls, Yu. M. Bunkov, E. Collin, H. Godfrin, and P. Sharma, Phys. Rev. B **72**, 024507 (2005).
[4] E. Collin, S. Triqueneaux, Yu. M. Bunkov, and H. Godfrin, Phys. Rev. B **80**, 094422 (2009).
[5] M. R. Freeman and R. C. Richardson, Phys. Rev. B **41**, 11011 (1990).
[6] S. M. Tholen and J. M. Parpia, Phys. Rev. Lett. **67**, 334 (1991); **68**, 2810 (1992).
[7] D. Kim, M. Nakagawa, O. Ishikawa, T. Hata, T. Kodama, and H. Kojima, Phys. Rev. Lett. **71**, 1581 (1993).
[8] S. C. Steel, J. P. Harrison, P. Zawadzki, and A. Sachrajda, J. Low Temp. Phys. **95**, 759 (1994).
[9] S. Murakawa, M. Wasai, K. Akiyama, Y. Wada, Y. Tamura, R. Nomura, and Y. Okuda, Phys. Rev. Lett. **108**, 025302 (2012).
[10] B. I. Barker, L. Polukhina, J. F. Poco, L. W. Hrubesh, and D. D. Osheroff, J. Low Temp. Phys. **113**, 635 (1998).
[11] B. I. Barker, Y. Lee, L. Polukhina, D. D. Osheroff, L. W. Hrubesh, and J. F. Poco, Phys. Rev. Lett. **85**, 2148 (2000).
[12] G. Gervais, K. Yawata, N. Mulders, and W. P. Halperin, Phys. Rev. B **66**, 054528 (2002).
[13] V. V. Dmitriev, V. V. Zavjalov, D. E. Zmeev, I. V. Kosarev, and N. Mulders, JETP Lett. **76**, 312 (2002).
[14] V. V. Dmitriev, I. V. Kosarev, N. Mulders, V. V. Zavjalov, and D. Ye. Zmeev, Physica (Amsterdam) **329B–333B**, 320 (2003).
[15] V. V. Dmitriev, D. A. Krasnikhin, N. Mulders, A. A. Senin, G. E. Volovik, and A. N. Yudin, JETP Lett. **91**, 599 (2010).
[16] J. Pollanen, J. I. A. Li, C. A. Collett, W. J. Gannon, and W. P. Halperin, Phys. Rev. Lett. **107**, 195301 (2011).
[17] D. T. Sprague, T. M. Haard, J. B. Kycia, M. R. Rand, Y. Lee, P. J. Hamot, and W. P. Halperin, Phys. Rev. Lett. **77**, 4568 (1996).
[18] A. Golov, J. V. Porto, and J. M. Parpia, Phys. Rev. Lett. **80**, 4486 (1998).
[19] E. V. Thuneberg, S. K. Yip, M. Fogelström, and J. A. Sauls, Phys. Rev. Lett. **80**, 2861 (1998).
[20] P. Sharma and J. A. Sauls, J. Low Temp. Phys. **125**, 115 (2001).
[21] R. Hänninen and E. V. Thuneberg, Phys. Rev. B **67**, 214507 (2003).
[22] K. Aoyama and R. Ikeda, Phys. Rev. B **73**, 060504 (2006).
[23] R. Ikeda, Phys. Rev. B **91**, 174515 (2015).
[24] K. Aoyama and R. Ikeda, J. Phys. Conf. Ser. **150**, 032005 (2009).
[25] G. Baramidze and G. Kharadze, Physica (Amsterdam) **284B–288B**, 305 (2000).
[26] J. A. Sauls and P. Sharma, Phys. Rev. B **68**, 224502 (2003).
[27] G. Baramidze and G. Kharadze, J. Low Temp. Phys. **135**, 399 (2004).
[28] J. A. Sauls and P. Sharma, New J. Phys. **12**, 083056 (2010).
[29] V. E. Asadchikov, R. Sh. Askhadullin, V. V. Volkov, V. V. Dmitriev, N. K. Kitaeva, P. N. Martynov, A. A. Osipov, A. A. Senin, A. A. Soldatov, D. I. Chekrygina, and A. N. Yudin, JETP Lett. **101**, 556 (2015).
[30] R.Sh. Askhadullin, V. V. Dmitriev, D. A. Krasnikhin, P. N. Martinov, L. A. Melnikovsky, A. A. Osipov, A. A. Senin, and A. N. Yudin, J. Phys. Conf. Ser. **400**, 012002 (2012).
[31] V. V. Dmitriev, L. A. Melnikovsky, A. A. Senin, A. A. Soldatov, and A. N. Yudin, JETP Lett. **101**, 808 (2015).
[32] J. A. Sauls, Phys. Rev. B **88**, 214503 (2013).
[33] I. A. Fomin, JETP **118**, 765 (2014).
[34] R.Sh. Askhadullin, V. V. Dmitriev, D. A. Krasnikhin, P. N. Martinov, A. A. Osipov, A. A. Senin, and A. N. Yudin, JETP Lett. **95**, 326 (2012).
[35] V. V. Dmitriev, A. A. Senin, A. A. Soldatov, E. V. Surovtsev, and A. N. Yudin, JETP **119**, 1088 (2014).
[36] V. V. Dmitriev, A. A. Senin, A. A. Soldatov, and A. N. Yudin, Phys. Rev. Lett. **115**, 165304 (2015).
[37] N. Zhelev, M. Reichl, T. S. Abhilash, E. N. Smith, K. X. Nguyen, E. J. Mueller, and J. M. Parpia, Nat. Commun. **7**, 12975 (2016).
[38] V. V. Volkov, V. V. Dmitriev, D. V. Zolotukhin, A. A. Soldatov, and A. N. Yudin, Instrum. Exp. Tech. **60**, 737 (2017).
[39] V. V. Dmitriev, I. V. Kosarev, D. V. Ponarin, and R. Scheibel, J. Low Temp. Phys. **113**, 945 (1998).
[40] H. Franco, J. Bossy, and H. Godfrin, Cryogenics **24**, 477 (1984).
[41] See Supplemental Material at http://link.aps.org/supplemental/10.1103/PhysRevLett.120.075301, which includes Refs. [42–44], for additional information about the samples and the ^{4}He coverage as well as for superfluid phase diagrams in nafen-90 and nafen-243.
[42] T. Herman, J. Day, and J. Beamish, Phys. Rev. B **73**, 094127 (2006).
[43] H. Kato, W. Miyashita, R. Nomura, and Y. Okuda, J. Low Temp. Phys. **148**, 621 (2007).
[44] V. M. T. Su, M. Terehov, and T. W. Clyne, Adv. Eng. Mater. **14**, 1088 (2012).
[45] G. E. Volovik, J. Low Temp. Phys. **150**, 453 (2008).
[46] R.Sh. Askhadullin, V. V. Dmitriev, P. N. Martynov, A. A. Osipov, A. A. Senin, and A. N. Yudin, JETP Lett. **100**, 662 (2015).
[47] M. R. Freeman, R. S. Germain, E. V. Thuneberg, and R. C. Richardson, Phys. Rev. Lett. **60**, 596 (1988).
[48] S. Autti, V. V. Dmitriev, J. T. Mäkinen, A. A. Soldatov, G. E. Volovik, A. N. Yudin, V. V. Zavjalov, and V. B. Eltsov, Phys. Rev. Lett. **117**, 255301 (2016).
[49] V. V. Dmitriev, A. A. Soldatov, and A. N. Yudin, J. Low Temp. Phys. **187**, 398 (2017).